BIOLOGY OF REPRODUCTION **80,** 897–904 (2009)
Published online before print 14 January 2009.
DOI 10.1095/biolreprod.108.075242

Localization of Low-Density Detergent-Resistant Membrane Proteins in Intact and Acrosome-Reacted Mouse Sperm[1]

Patricia V. Miranda,[3,4] Alicia Allaire,[3] Julian Sosnik,[3] and Pablo E. Visconti[2,3]

Department of Veterinary and Animal Sciences,[3] University of Massachusetts, Amherst, Massachusetts
Instituto de Biologia y Medicina Experimental,[4] CONICET, Buenos Aires, Argentina

ABSTRACT

Mammalian sperm become fertile after completing capacitation, a process associated with cholesterol loss and changes in the biophysical properties of the sperm membranes that prepares the sperm to undergo the acrosome reaction. Different laboratories have hypothesized that cholesterol efflux can influence the extent and/or movement of lipid raft microdomains. In a previous study, our laboratory investigated the identity of sperm proteins putatively associated with rafts. After extraction with Triton X-100 and ultracentrifugation in sucrose gradients, proteins distributing to the light buoyant-density fractions were cored from polyacrylamide gels and microsequenced. In this study, a subset of these proteins (TEX101, basigin, hexokinase 1, facilitated glucose transporter 3, IZUMO, and SPAM1) and other molecules known to be enriched in membrane rafts (caveolin 2, flotillin 1, flotillin 2, and the ganglioside GM3) were selected to investigate their localization in the sperm and their behavior during capacitation and the acrosome reaction. These molecules localize to multiple sperm domains, including the acrosomal cap (IZUMO, caveolin 2, and flotillin 2), equatorial segment (GM3), cytoplasmic droplet (TEX101), midpiece (basigin, facilitated glucose transporter 3, and flotillin 2), and principal piece (facilitated glucose transporter 3). Some of these markers modified their immunofluorescence pattern after sperm incubation under capacitating conditions, and these changes correlated with the occurrence of the acrosome reaction. While GM3 and caveolin 2 were not detected after the acrosome reaction, flotillin 2 was found in the equatorial segment of acrosome-reacted sperm, and IZUMO distributed along the sperm head, reaching the post- and para-acrosomal areas. Taking into consideration the requirement of the acrosome reaction for sperm to become fusogenic, these results suggest that membrane raft dynamics may have a role in sperm-egg membrane interaction.

acrosome reaction, fertilization, flotillin, IZUMO, lipid rafts, signal transduction, sperm, sperm capacitation

INTRODUCTION

Mammalian sperm are highly specialized cells that undergo a complex series of differentiating processes to become fertile. These processes start in the male reproductive tract with epididymal maturation and continue in the female tract, where sperm undergo capacitation and become fully able to fertilize an oocyte [1, 2]. Molecular events implicated in the initiation of capacitation include lipid rearrangements in the sperm plasma membrane that are coupled to changes in ion fluxes and to several signaling cascades. Among the changes in lipids, capacitation has long been thought to involve loss of cholesterol, leading to a different organization of the sperm plasma membrane.

The release of cholesterol appears to be necessary for the signaling events that accompany capacitation [3–5], including the preparation of the sperm to undergo an agonist-induced acrosome reaction. However, our understanding of how sterol efflux couples to the regulation of signal transduction pathways intrinsic to capacitation remains rudimentary. Years after the description of the plasma membrane fluid mosaic model [6], specialized platforms clustering signaling molecules were identified [7]. These structures are highly enriched in cholesterol and glycosphingolipids; this lipid composition provides their characteristic biochemical properties (insolubility in nonionic detergents such as Triton X-100 at 4°C and light buoyant density after centrifugation in a sucrose gradient). Although several limitations should be taken into account [8], sucrose light buoyant detergent-resistant membranes (DRMs) have been widely used as a first approach to identify membrane rafts [9–15]. Current concepts attribute important signaling properties to the existence of membrane rafts acting to bring protein assemblies together [16–18]. In the case of mammalian sperm, it has been hypothesized that cholesterol release during capacitation modifies the function/location of proteins in sperm raft microdomains [19–24]. In an effort to elucidate the mechanisms by which the release of cholesterol couples to signaling events in the sperm, we previously conducted a proteomic analysis of the sperm light buoyant fractions and identified a number of proteins, including hexokinase 1 (HK1), testis serine proteases 1 and 2, TEX101, hyaluronidase (SPAM1), facilitated glucose transporter 3 (SLC2A3), lactate dehydrogenase A, carbonic anhydrase IV, IZUMO, pantophysin, basigin (BSG), and CRISP1 [20].

Sperm are highly polarized cells, and their membranes can be categorized into different compartments. In intact sperm, the plasma membrane on the head surrounds the anterior acrosome, the equatorial segment, and the postacrosomal region. In the tail, the membrane covers the anterior part of the flagellum (midpiece) containing the mitochondria and the posterior portion of the tail (principal piece) containing the fibrous sheath surrounding the outer dense fibers [25]. These sperm compartments should be taken into account when the role of DRM proteins is analyzed; therefore, in this study we used antibodies against a subset of these proteins to investigate their localization in mouse sperm and their behavior during capacitation. Using filipin staining, the cholesterol-rich regions have been mapped to the plasma membrane overlaying the acrosome [5, 26, 27]. However, our findings indicate that

[1]Supported by the Eunice Kennedy Shriver National Institute of Child Health and Human Development grants NIH HD38082 and NIH HD44044 (to P.E.V.).
[2]Correspondence: Pablo E. Visconti, Department of Veterinary and Animal Sciences, University of Massachusetts, Amherst, MA 01003. FAX: 413 545 6326; e-mail: pvisconti@vasci.umass.edu

Received: 3 December 2008.
First decision: 16 December 2008.
Accepted: 17 December 2008.

eISSN: 1259-7268 http://www.biolreprod.org
ISSN: 0006-3363

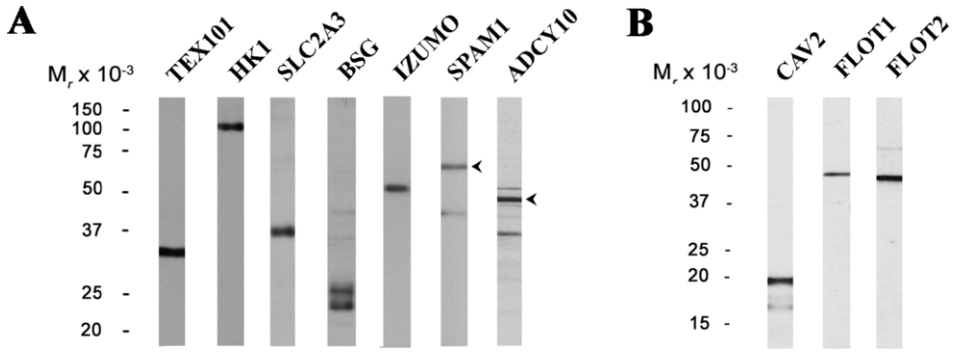

FIG. 1. Specificity of antibodies directed toward DRMs and other sperm proteins. Total sperm extracts were prepared as detailed in *Materials and Methods,* separated using 10% (**A**) or 15% (**B**) acrylamide gels and analyzed by Western blot using different antibodies directed against the corresponding proteins. Arrowheads represent bands highlighted in Figure 2.

proteins present in the light buoyant fractions, as well as other molecules known to distribute dynamically in membrane rafts, localized in multiple sperm compartments, including the anterior head, equatorial segment, cytoplasmic droplet, midpiece, and principal piece. When the behavior of these molecules during capacitation was studied, no changes were found in the tail-resident proteins. On the other hand, while some of the molecules in the head were lost, others change their immunofluorescence pattern; these changes were observed only in sperm that had undergone acrosomal exocytosis. IZUMO, present exclusively in the acrosomal region in intact sperm, spread to the post- and para-acrosomal regions of the sperm head in acrosome-reacted cells, while flotillin 2 (FLOT2), originally in the dorsal acrosome and midpiece, appeared in the equatorial segment. Considering that sperm acquire fusogenic capacity after the acrosome reaction, these changes in DRM-associated proteins could indicate their involvement in sperm-egg interaction.

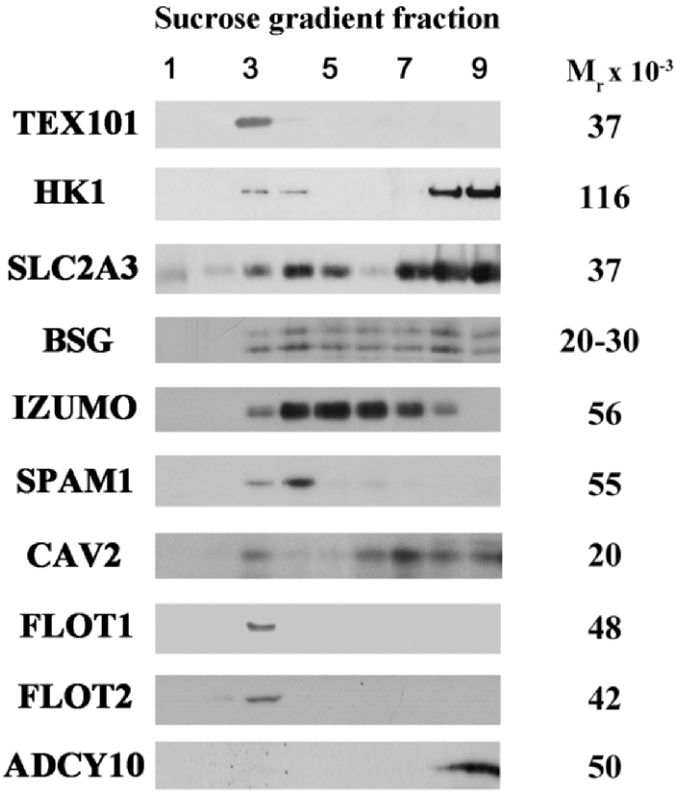

FIG. 2. Distribution of proteins along the sucrose gradient. Sperm were extracted with 0.5% Triton X-100 and subjected to ultracentrifugation on a sucrose gradient as described in *Materials and Methods*. Nine fractions were collected from top to bottom and were analyzed by SDS-PAGE and Western blot using different antibodies. The molecular weights of the bands shown are in the right column. In the case of SPAM1 and ADCY10, bands shown are those marked with an arrowhead in Figure 1. A nonraft protein (ADCY10) was included as control.

MATERIALS AND METHODS

Materials

All chemicals were reagent grade and were purchased from Sigma or Fisher unless otherwise stated. Molecular weight standards and all reagents used for SDS-PAGE were from BioRad. The following protease inhibitors were obtained from Sigma: PMSF, benzamidine, Nα-tosyl-L-lysine chloromethyl ketone (TLCK), mammalian cell and tissue extracts cocktail 4-(2-aminoethyl)benzenesulfonyl fluoride hydrochloride (AEBSF), aprotinin, bestatin, N-(trans-epoxysuccinyl)-L-leucine 4-guanidinobutylamide (E-64), leupeptin, and pepstatin A. Calcium ionophore A23187 was from Calbiochem. Fluorescent reagents purchased from Molecular Probes included anti-rabbit IgG, anti-mouse IgG, anti-mouse IgM, and peanut agglutinin lectin (PNA) conjugated to Alexa Fluor 555 or 488. Peroxidase-conjugated anti-rabbit IgG (Sigma) and anti-mouse IgG (Jackson ImmunoResearch Laboratories) were used for Western blot analyses.

Antibodies

Specific antibodies directed against the different molecules analyzed in this study were obtained from several commercial and noncommercial sources as detailed herein. Monoclonal anti-TEX101 was generously provided by Dr. Yoshihiko Araki from Yamagata University (Yamagata, Japan). Dr. John Wilson from Michigan State University (East Lansing, MI) contributed the rabbit anti-HK1. Polyclonal anti-IZUMO was a gift from Dr. Masaru Okabe at Osaka University (Osaka, Japan). A specific polyclonal antiserum recognizing SPAM1 was obtained from Dr. Diana Myles and Dr. Paul Primakoff at the University of California, Davis. The antibody recognizing SLC2A3 was purchased from Alpha Diagnostic International. Dr. Kenji Kadomatsu from Nagoya University (Nagoya, Japan) generously provided the anti-BSG. Monoclonal antibodies reacting against FLOT1 and FLOT2 were purchased from BD Biosciences. Anti-CAV2 was obtained from Santa Cruz Biotechnology Inc. The monoclonal IgM that specifically recognizes the ganglioside GM3 was purchased from Seikagaku Corporation. Dr. Lonny Levin and Dr. Jochen Buck from the Department of Pharmacology, Weill Medical College of Cornell University (New York, NY) provided the antibody R2, which reacts against bicarbonate-dependent cyclase (ADCY10).

Sperm Preparation

Mouse sperm were collected from CD1 retired male breeders (Charles River), euthanized in accord with Institutional Animal Care and Use Committee guidelines and following experimental protocols previously approved by the Animal Care Committee of the University of Massachusetts. For the sperm to swim out, the cauda epididymis from each animal was placed in 0.5 ml of modified Whitten-Hepes medium (WH) containing 100 mM NaCl, 4.7 mM KCl, 1.2 mM KH_2PO_4, 1.2 mM $MgSO_4$, 5.5 mM glucose, 1 mM Pyruvic acid, 4.8 mM L(+)-lactic acid hemicalcium salt in 20 mM Hepes, pH 7.3, at 37°C. After 10 min, sperm suspension was diluted into capacitating media or collected and centrifuged at 500 × *g* for 5 min at room temperature (RT). For capacitation, 50 μl of the original suspension was diluted into 450 μl of capacitating media (WH supplemented with 20 mM $NaHCO_3$ and 3 mg/ml of bovine serum albumin [BSA], A-0281; Sigma) and incubated for 60 min as previously described [28]. To induce the acrosome reaction, capacitated sperm were treated with 3 μM calcium ionophore A23187 for 30 min.

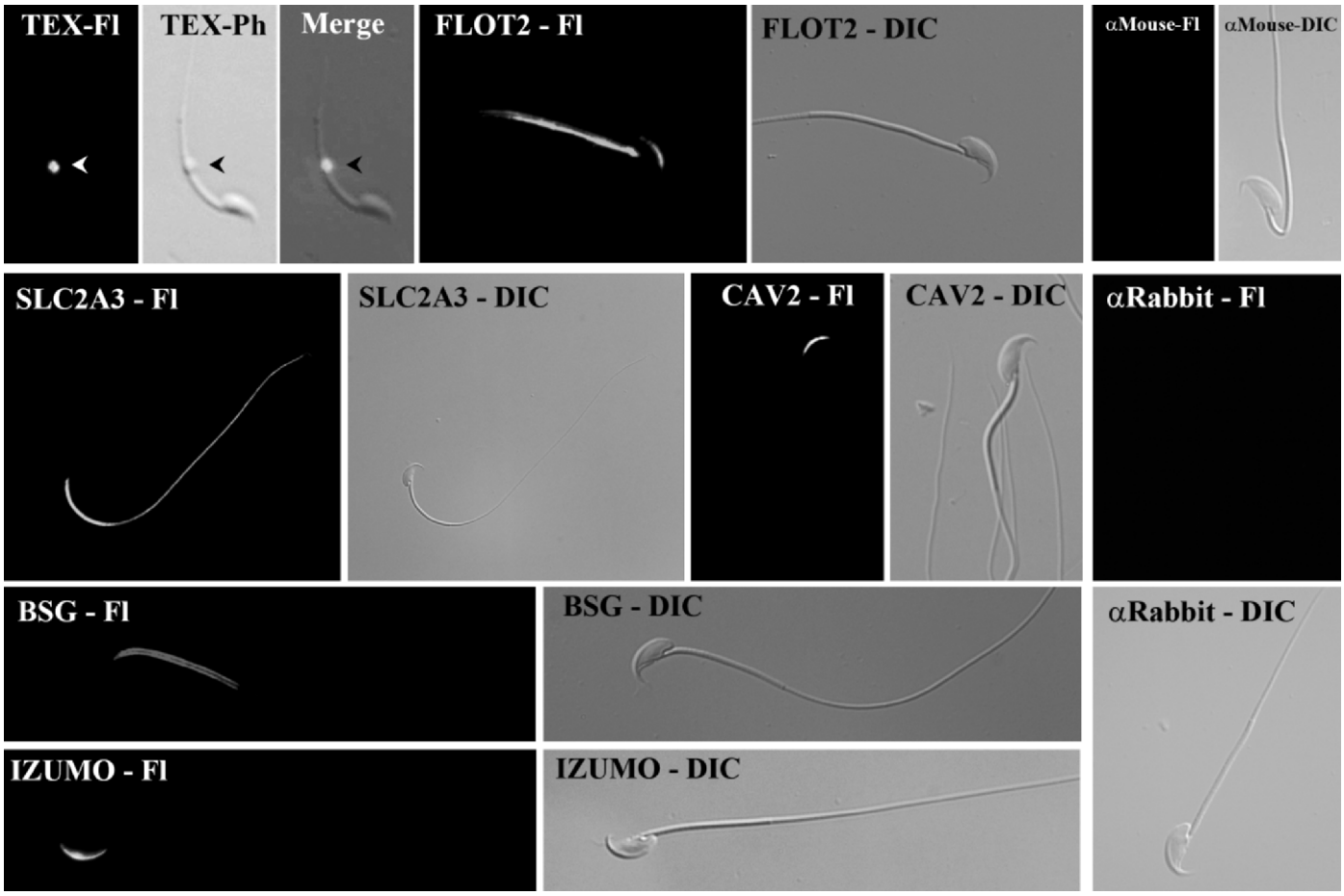

FIG. 3. Location of DRM proteins among the different sperm compartments. Mouse sperm were fixed with 2% formaldehyde, immobilized on slides, and permeabilized with 0.1% Triton X-100. Cells were incubated overnight with different antibodies raised in mouse (anti-TEX and anti-FLOT2) or rabbit (anti-SLC2A3, anti-CAV2, anti-BSG, and anti-IZUMO), followed by the respective Alexa Fluor-conjugated secondary antibody. Primary antibodies were omitted as control (αMouse and αRabbit panels). Illustrations represent the images obtained under fluorescence (Fl) or transmitted light illumination (Ph, phase contrast; DIC, differential interference contrast). Experiments were repeated at least three times; representative sperm are shown. Arrowheads represent cytoplasmic droplet. Original magnification ×60.

Isolation of Light Buoyant-Density DRM Fractions

Sperm suspensions were centrifuged at 500 × *g* for 10 min and washed with WH medium. The pellet was resuspended in 400 μl of TEN buffer (25 mM Tris-HCl, 150 mM NaCl, 5 mM edetic acid, pH 7.3) supplemented with 0.5% Triton X-100 and a protease inhibitor cocktail (1 mM PMSF, 1 mM NaF, 2 mM sodium orthovanadate, 20 μg/ml of leupeptin, 15 μg/ml of pepstatin, 0.8 mM aprotinin, 10 mM benzimidine, 3 μg/ml of TLCK, 1 mM AEBSF, 40 μM bestatin, and 14 μM E-64). This suspension was Dounce homogenized and sonicated with five brief bursts of 1 sec each. Samples were kept on ice for 5 min and then rotated at 4°C for 45 min. Lysates were adjusted to 40% sucrose with the addition of 400 μl of 80% sucrose in TEN buffer and placed in the bottom of a 2-ml Beckman centrifuge tube. This suspension was gently overlaid with 800 μl of 30% sucrose in TEN buffer, followed by 400 μl of 5% sucrose in TEN buffer. The samples were then centrifuged at 200 000 × *g* for 18 h in a TLS 55 swinging bucket rotor in a Beckman Optima-TLX ultracentrifuge. After centrifugation, 200-μl fractions were carefully collected from the top to the bottom of the gradient. Fractions were prepared for SDS-PAGE by the addition of 0.2 volumes of 5× nonreducing Laemmli buffer, boiled for 5 min, and kept frozen until use.

SDS-PAGE and Western Blot

Total sperm extracts were obtained by cell suspension in nonreducing Laemmli buffer and by boiling for 5 min. Before running, samples were supplemented with 5% β-mercaptoethanol when required. The SDS-denaturing gels of different acrylamide concentrations (10% or 15%) were used depending on the protein under study. After electrophoresis, proteins were electroblotted to polyvinylidene fluoride membrane and blocked with 5% skimmed milk. All incubation and washing procedures were done with PBS supplemented with 0.1% Tween 20 (PBST). Membranes were blocked for 1 h at RT and then incubated with the different first antibodies overnight at 4°C as previously described [29]. After washing three times for 5 min, the specific peroxidase-conjugated secondary antibody was added, and incubation was carried out for 1 h at RT. The membranes were washed with PBST, and immune complexes were located using ECL Plus and Kodak Biomax light films.

Immunocytochemistry

Sperm were fixed in suspension by the addition of fresh formaldehyde (prepared from paraformaldehyde [final concentration, 2%]) and incubation for 30 min at 4°C. After washing two times with PBS, sperm were immobilized on slides and air dried. Cells were permeabilized with 0.1% Triton X-100 and 0.2% formaldehyde for 5 min at RT. After washing with PBS, blocking was done by 30-min incubation with 1% BSA in PBS. Primary antibodies were diluted in PBS supplemented with 0.1% BSA and incubated overnight at 4°C. After washing with PBS, cells were incubated with the respective Alexa Fluor-conjugated secondary antibody for 60 min at RT. When double staining was required, PNA coupled to Alexa Fluor 488 was included in the solution of the secondary antibody. After washing, cells were mounted using Slow Fade (Molecular Probes).

RESULTS

Validation of Antibodies and Confirmation of Sperm DRM-Resident Proteins by Western Blot

We previously identified a number of proteins using a combination of one-dimensional PAGE and tandem mass

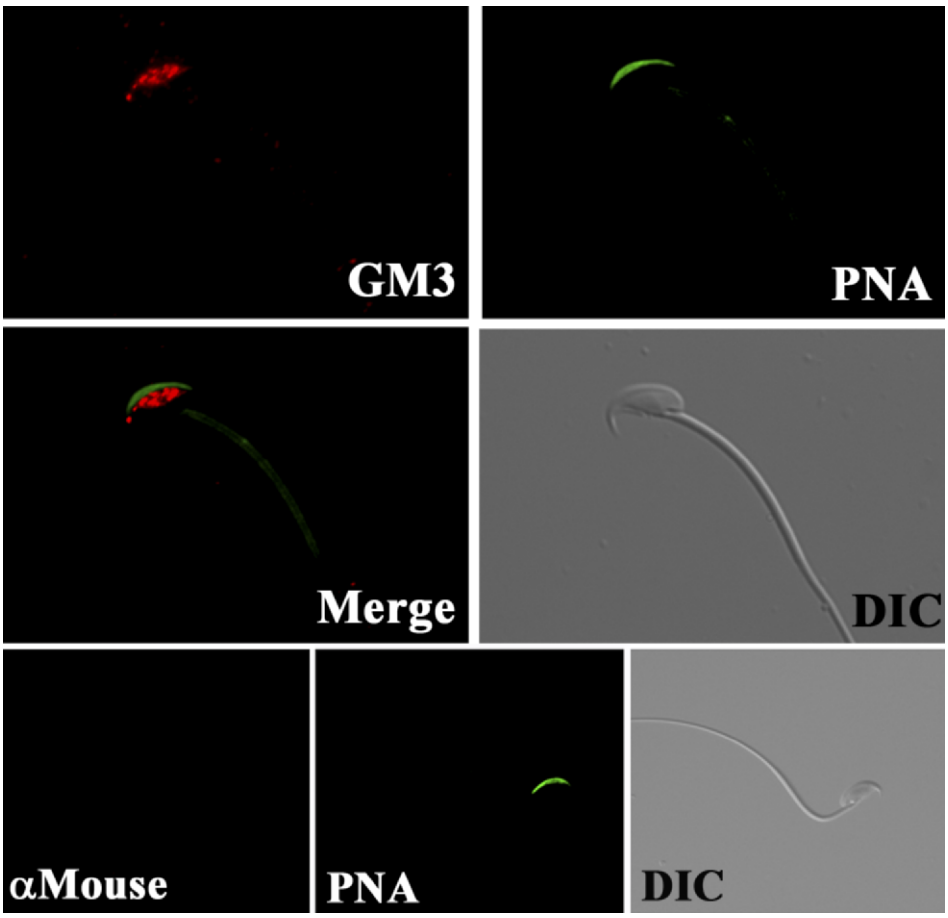

FIG. 4. Detection of ganglioside GM3 in mouse sperm. Mouse sperm fixed and permeabilized as already described were incubated overnight with a monoclonal anti-GM3 antibody, followed by Alexa Fluor 555-conjugated secondary antibody (GM3). Cells were also stained with Alexa Fluor 488-conjugated PNA. No primary antibody controls were used (lower panels). Experiments were repeated at least three times; representative sperm are shown. DIC, differential interference contrast. Original magnification ×60.

spectrometry of DRM fractions after separation in a sucrose gradient [20]. To confirm their association with the light-density fractions, antibodies against these proteins were obtained from different commercial and noncommercial sources as enumerated in *Materials and Methods*. Each of these antibodies was validated by Western blot of total sperm extracts as shown in Figure 1A, and the antibodies recognized proteins of the predicted molecular weight. In addition to the proteins identified previously [20], we assayed for the presence of other proteins known to be enriched in membrane rafts in many cell types such as CAV2, FLOT1, and FLOT2. Antibodies against these proteins react with polypeptides of the expected molecular weight, indicating the presence of these proteins in mouse sperm (Fig. 1B). We also tested antibodies against ADCY10, a nonraft protein.

The validated antibodies were then used to probe Western blots of sucrose gradient fractions obtained as described in *Materials and Methods* (Fig. 2). Among the assayed proteins, it was possible to distinguish three different gradient distributions. Although all of them were found in the light fraction used previously for tandem mass spectrometry identification [20], TEX101, SPAM1, FLOT1, and FLOT2 were present exclusively in the light fractions; IZUMO was more widespread and was also found in intermediate-density fractions; and a third set of proteins comprising SLC2A3, BSG, HK1, and CAV2 was found in most fractions, including the heavy ones. ADCY10 distributed exclusively in the heavy fractions.

DRM-Resident Proteins Compartmentalized to Different Sperm Regions

A unique feature of sperm cells is the subdivision of the plasma membrane into well-defined regional domains with different compositions and functions [25]. In addition to the domains described in the *Introduction*, the cytosolic droplet that is present in a fraction of cauda epididymal mouse sperm constitutes another level of complexity. To analyze the specific distribution of the sperm DRM proteins in the different membrane regions, the already-validated antibodies were used to localize the respective proteins by immunofluorescence. As shown in Figure 3, DRM proteins were found in the anterior head (IZUMO, CAV2, and FLOT2), midpiece (SLCA3, FLOT2, BSG, and SLC2A3), and principal piece (SLC2A3). TEX101, a protein that localized exclusively to the light buoyant sucrose gradient fractions, was present only in the cytoplasmic droplet.

In addition to the proteins enriched in membrane rafts, DRMs are enriched in gangliosides. Recently, fluorescently labeled cholera toxin has been used to address the presence of GM1 in sperm from different mammalian species [19, 21, 23, 30–33]. Although GM1 is the best studied in sperm, other gangliosides are known to be enriched in membrane rafts [34], and differential ganglioside distribution among these membrane microdomains has been reported [35–37]. In particular, GM3 appears to be the major ganglioside in the male reproductive system [38], and several studies [39–41] demonstrate its abundance in bovine, ovine, and human sperm. However, localization of GM3 on sperm has not yet been analyzed, to our knowledge. To investigate the location of GM3 in mouse sperm, a specific anti-GM3 antibody was tested by immunofluorescence. This monoclonal antibody has been validated by Kotani et al. [42, 43] and was used in several studies [35, 44–48]. Anti-GM3 fluorescent signal was found to be restricted to the equatorial segment (Fig. 4), whereas PNA signal exclusively stained the anterior acrosomal region.

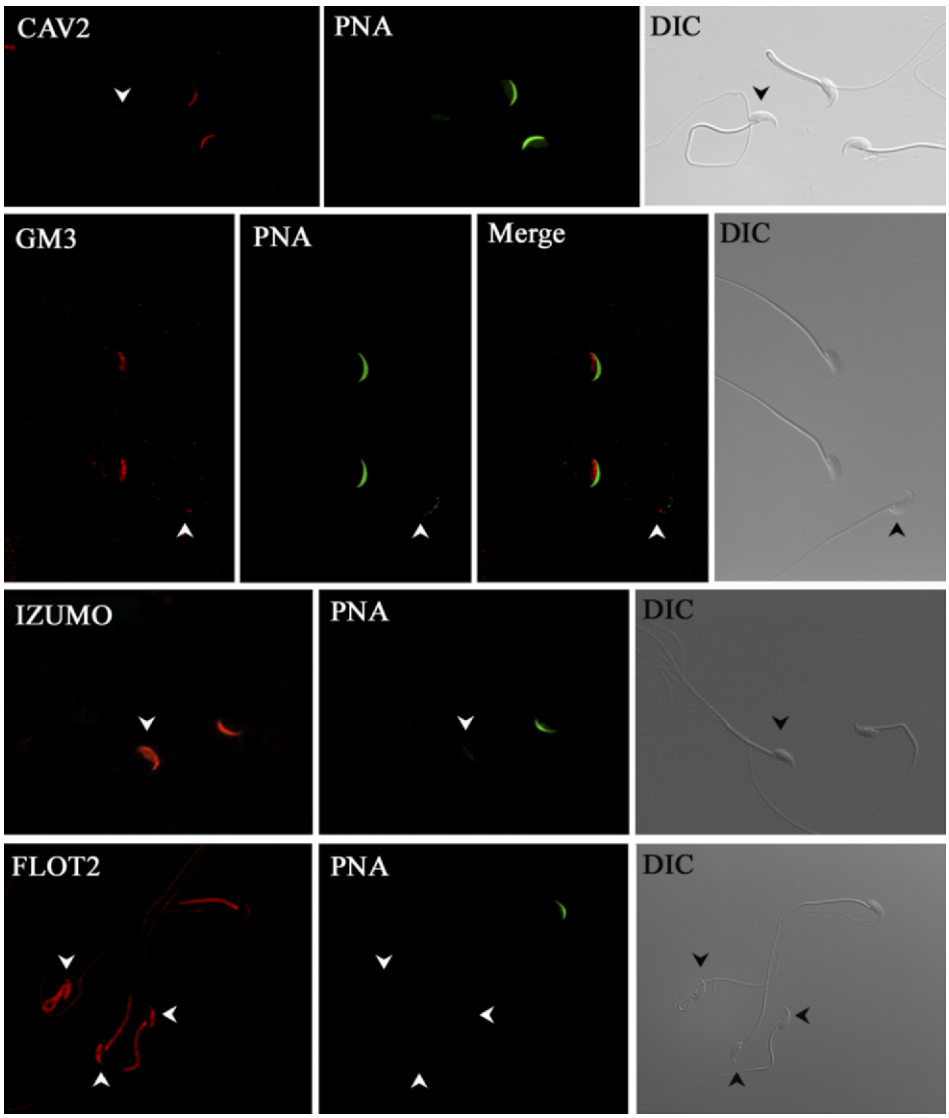

FIG. 5. Differential immunofluorescence pattern of GM3, CAV2, IZUMO, and FLOT2 in capacitated sperm. Mouse sperm incubated under capacitating conditions were analyzed by immunofluorescence as described in *Materials and Methods* using anti-GM3, anti-CAV2, anti-IZUMO, and anti-FLOT2, followed by the respective Alexa Fluor 555-conjugated secondary antibody. Cells were also stained with Alexa Fluor 488-conjugated PNA to relate the staining patterns to the acrosomal status. Sperm that underwent the acrosome reaction correspond to those showing the new staining patterns (arrowheads). Experiments were repeated at least three times; representative sperm are shown. DIC, differential interference contrast. Original magnification ×60.

Sperm Acrosome Reaction Correlates with Changes in DRM Protein Immunolocalization

As previously stated, cholesterol content is relevant for the function of raft proteins and for sperm capacitation. To analyze if there was any relationship between these two events, we studied DRM proteins after incubating sperm under capacitating conditions. Most of the proteins did not change their respective immunofluorescence pattern upon incubation (data not shown). However, some proteins (IZUMO, CAV2, and FLOT2) and the ganglioside GM3 showed two different staining patterns in the capacitated population as shown in Figure 5. In the case of CAV2 and GM3, some sperm displayed no signal; in contrast, FLOT2 and IZUMO showed a different staining pattern. Although these changes were observed in the capacitated population, in all cases they correlated with the loss of PNA staining, suggesting that the differential immunofluorescence patterns were due to the acrosome reaction and were not directly related to capacitation.

To further confirm this observation, the immunolocalization of FLOT2 and IZUMO was studied after inducing the acrosome reaction with the calcium ionophore A23187. As shown in Figure 6, sperm that have lost PNA staining showed a new IZUMO localization. Although both FLOT2 and IZUMO displayed a different staining pattern in acrosome-reacted cells versus intact sperm, they did not colocalize (data not shown). While FLOT2 was restricted to the equatorial segment, IZUMO distributed into adjacent regions.

DISCUSSION

Capacitation has been associated with changes in the lipid composition of the sperm plasma membrane; in particular, cholesterol efflux induces signaling events in the sperm, including the capacitation-associated increase in tyrosine phosphorylation and the preparation of the sperm to undergo the acrosome reaction [1, 5]. Previous work from our group has used a proteomic analysis of low-density DRM-resident proteins in an effort to investigate whether cholesterol efflux regulates membrane rafts during sperm capacitation [20]. The use of detergent to relate protein association to rafts is the most widely used method to analyze the composition of membrane rafts and to identify putative resident proteins [9–14]. However, this procedure has been questioned on the basis that detergent can induce the formation of membrane domains and fails to provide physiologically relevant information [8, 14]. Despite these criticisms, detergent separation can still be considered a first approach to determining components of membrane rafts. In particular, although proteins not belonging to rafts could be found in the low-density DRM fractions, it is

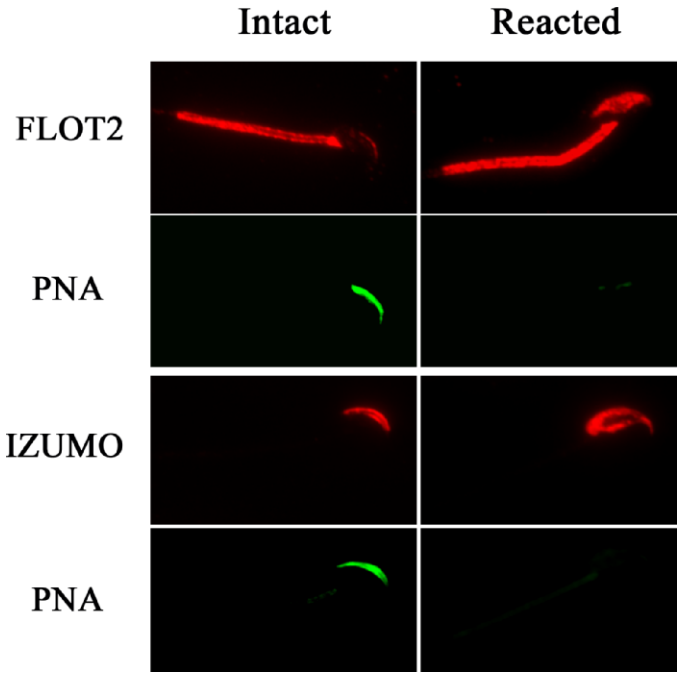

FIG. 6. Differential location of FLOT2 and IZUMO in intact and acrosome-reacted sperm. Mouse sperm were analyzed by immunofluorescence with anti-FLOT2 or anti-IZUMO before or after capacitation and treatment with the calcium ionophore A23187. Cells were also stained with Alexa Fluor 488-conjugated PNA to check for the acrosomal status. Experiments were repeated al least three times; representative sperm are shown. Original magnification ×60.

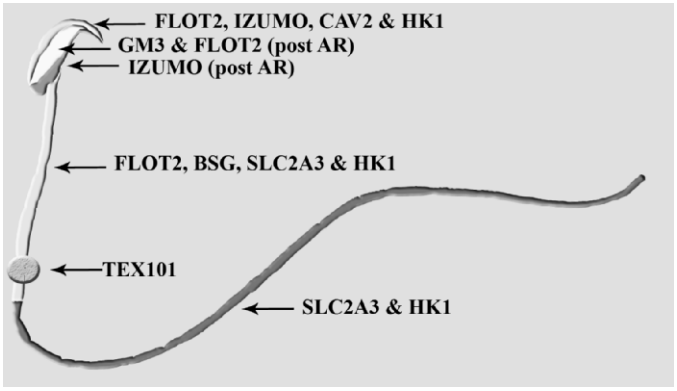

FIG. 7. Schematic representation of the distribution of DRM proteins in sperm compartments depicting the results obtained using the antibodies directed against the different DRM-resident molecules analyzed in the study; HK1 localization as described previously [49] is also shown. As already noted in the text, IZUMO and FLOT2 demonstrate a different immunofluorescence pattern after the acrosome reaction (AR).

generally believed that most proteins associated with membrane rafts will behave as detergent resistant [8]. In addition, an essential property of sperm cells is their highly compartmentalized structure [25]. Taking this into consideration, an alternative experimental approach is required to determine the original location of DRM proteins among the different sperm compartments.

In the present work, we chose a series of DRM-resident proteins to investigate their localization in sperm. These proteins were not restricted to one sperm region but were distributed among different sperm compartments; our findings regarding localization of these proteins are illustrated in Figure 7. Some of these molecules (e.g., CAV2, GM3, IZUMO, and FLOT2) change their localization during the acrosome reaction. While CAV2 and GM3 appear to be lost, IZUMO and FLOT2 show a different pattern of localization in a fraction of the capacitated sperm population. The new patterns were found only in acrosome-reacted sperm, suggesting that the changes were due not to capacitation but to the acrosome reaction.

Sphingolipids are derivatives of the long-chain amino alcohols sphingosine and dihydrosphingosine. The sphingoid long-chain base is linked to a fatty acid molecule via an amide bond-forming ceramide. The addition of carbohydrates to this ceramide backbone leads to the formation of a great diversity of glycosphingolipids, including the gangliosides GM1 and GM3 that differ only in their oligosaccharide chains. Like cholesterol, sphingolipids are found to be enriched in membrane rafts; this behavior is due to the presence of two long saturated alkyl chains that can be organized and condensed by sterols to form the liquid-ordered phase of membrane rafts [49]. In sperm, other investigations on nonprotein raft markers have focused on GM1. Using cholera toxin, this ganglioside was shown to localize to the plasma membrane overlaying the acrosome in living sperm [32]. On the other hand, using biochemical methods, it has been demonstrated by biochemical methods that GM3 is the most abundant ganglioside in the male reproductive tract and in sperm [39–41]; however, localization of GM3 in these cells was undetermined. In this study, we used previously validated antibodies against GM3 [42, 43] to determine the immunofluorescence pattern of this ganglioside in sperm and found it to be restricted to the equatorial segment.

Considering the method used in our original study [20], the source of the proteins located in the light-density fractions could belong to more than one membrane. In addition to the aforementioned sperm compartments (e.g., head and tail), the subcellular structure of the sperm encompasses different membranes, including the plasma membrane, outer acrosomal and inner acrosomal membranes, and nuclear and mitochondrial membranes. Although results obtained from the proteomic analysis suggested the absence of mitochondria and nuclear membranes in the sperm light-density fractions, DRM proteins coming from the inner and outer acrosomal membranes were also found in these fractions. The results of this study are in agreement with this possibility and with the assorted origin of plasma membranes contributing to the light-density fractions. In the tail, localization of BSG, SLC2A3, and FLOT2 suggests that DRM can be found along the different sections comprising the sperm flagella. The results in this study provide some other insightful clues for the sperm head. IZUMO cannot be detected on live sperm and is only exposed when plasma membrane integrity is disrupted by freezing, permeabilization, or the acrosome reaction [50, 51]; accordingly, it is hypothesized that this protein localizes to the inner acrosomal membrane. In this respect, the association of IZUMO with the light-density fraction provides evidence that the inner acrosomal membrane contributes to the total light buoyant DRM fractions. Even an ephemeral structure like the cytoplasmic droplet seems to preserve DRMs, as suggested by the highly restricted location of TEX101 in the light-density fractions and by the results of the immunofluorescence studies. These results confirm studies [37, 49] supporting the heterogeneity of DRMs with regard to their protein and lipid composition.

Pursuing our analysis on the putative involvement of DRM-resident proteins in sperm function, the location of selected proteins associated with the light-density fractions was reanalyzed in sperm incubated under capacitating conditions.

Although no relevant changes were noticed with capacitation, modifications in the immunofluorescence pattern of some proteins were observed in acrosome-reacted sperm. The acrosome reaction involves an extensive reorganization of the membranes located in the anterior head of the sperm cell. Multiple fusion points between the plasma and outer acrosomal membranes induce a fenestration process during which the components originally located in the apical portion of the sperm are lost [1]. After fusion, the inner acrosomal and plasma membranes become continuous, assembling a new sperm surface resulting from the mixing of their respective components. Caveolin 2, originally found in the anterior head of the sperm, could not be detected after the acrosome reaction, suggesting that this antigen is likely located at the plasma membrane covering the acrosomal cap and is consequently lost during exocytosis. In the case of GM3, although no signal was found on reacted sperm, the original localization of this ganglioside did not predict this behavior because the equatorial segment is excluded from the vesiculization process that takes place during the acrosome reaction [1]. Although the possible loss of GM3 cannot be ruled out, considering that anti-GM3 recognizes the glycoside portion of the GM3 molecule [42], the lack of signal of acrosome-reacted sperm could also be due to the removal of the respective epitope by acrosomal glycosidases released during exocytosis [1].

In contrast to CAV2 and GM3, the other two proteins analyzed, IZUMO and FLOT2, can still be detected by immunofluorescence in acrosome-reacted sperm, although they showed a different localization compared with the one originally displayed in nonreacted cells. In intact sperm, IZUMO was restricted to the dorsal portion of the sperm head; after the acrosome reaction, it distributed to a new region opposite to the anterior acrosome, including part of the postacrosomal region. Different IZUMO staining patterns have been previously observed [50], but their connection with antigen relocation due to the acrosome reaction has not been analyzed in detail. Concerning FLOT2, the staining formerly observed in the midpiece did not change with the acrosome reaction, but the signal located in the apical portion of the head extended along the acrosomal domain, revealing the presence of FLOT2 in the equatorial segment in cells that underwent the acrosome reaction. In addition to FLOT2, several proteins that have been reported to relocate after the acrosome reaction such as SPAM1, CRISP1, and IZUMO are present in the light buoyant DRM fractions [51–53]. This common feature suggests that changes in localization could be related to these membrane substructures rather than to a specific aspect of the individual proteins.

Although both IZUMO and FLOT2 change their location after the acrosome reaction, they do not seem to colocalize. While FLOT2 is restricted to the equatorial segment, IZUMO can move farther, crossing to the ventral para-acrosomal sperm domains. These compartments are separated by a specialized structure that seems to be defined during epididymal maturation and involves tyrosine phosporylation [54]. Other proteins reported to redistribute after the acrosome reaction are localized to the equatorial segment and are not able to pass the postacrosomal boundary [52, 53]. This suggests that protein redistribution after the acrosome reaction is a regulated process that may comprise a particular mechanism for IZUMO. It is a matter to be resolved why only IZUMO among all the proteins that move after the acrosome reaction is able to cross the postacrosomal boundary and whether this has a functional significance considering its relevance in sperm-egg fusion [55].

The membrane reorganization taking place during the acrosome reaction involves an additional change of high functional significance: the sperm becomes capable of fusing with the egg. Although IZUMO has been shown to be necessary for sperm-egg fusion [55], the molecular mechanisms conferring fusogenic ability to sperm are not well understood. Membrane microdomains and their resident molecules have been implicated in processes requiring cell-cell fusion such as invasion [56, 57]. With respect to the molecules depicting a different inmmunofluorescence pattern after the acrosome reaction, while FLOT2 has been positively correlated with metastatic processes [58], GM3 has been negatively associated with cell motility and invasiveness [59]. In the sperm, we can speculate that the presence of GM3 is associated with a nonfunctional equatorial segment and that GM3 modification or loss may be needed for the sperm to acquire the ability to fuse with the egg. Taking into consideration that IZUMO has a direct role in sperm-egg fusion as suggested by the null mutant phenotype [55], the putative participation of those regions where IZUMO localized after the acrosome reaction in sperm-egg fusion should be reanalyzed.

ACKNOWLEDGMENTS

We would like to thank Dr. Yoshihiko Araki (Yamagata University, Yamagata, Japan) for providing us with anti-TEX101, Dr. John Wilson (Michigan State University, East Lansing, MI) for the anti-HK1, Dr. Masaru Okabe (Osaka University, Osaka, Japan) for the anti-IZUMO, Dr. Diana Myles and Dr. Paul Primakoff (University of California, Davis) for the anti-SPAM1, Dr. Kenji Kadomatsu (Nagoya University, Nagoya, Japan) for providing the anti-BSG, and Dr. Lonny Levin and Dr. Jochen Buck (Weill Medical College of Cornell University, New York, NY) for the antibody against the bicarbonate-dependent cyclase.

REFERENCES

1. Yanagimachi R. Mammalian fertilization. In: Knobil E, Neill JD (eds.), The Physiology of Reproduction, vol. 1, 2nd ed. New York: Raven Press; 1994:189–317.
2. Visconti PE, Kopf GS. Regulation of protein phosphorylation during sperm capacitation. Biol Reprod 1998; 59:1–6.
3. Visconti PE, Bailey JL, Moore GD, Pan D, Olds-Clarke P, Kopf GS. Capacitation of mouse spermatozoa, I: correlation between the capacitation state and protein tyrosine phosphorylation. Development 1995; 121: 1129–1137.
4. Visconti PE, Moore GD, Bailey JL, Leclerc P, Connors SA, Pan D, Olds-Clarke P, Kopf GS. Capacitation of mouse spermatozoa, II: protein tyrosine phosphorylation and capacitation are regulated by a cAMP-dependent pathway. Development 1995; 121:1139–1150.
5. Visconti PE, Ning X, Fornes MW, Alvarez JG, Stein P, Connors SA, Kopf GS. Cholesterol efflux-mediated signal transduction in mammalian sperm: cholesterol release signals an increase in protein tyrosine phosphorylation during mouse sperm capacitation. Dev Biol 1999; 214:429–443.
6. Singer SJ, Nicolson GL. The fluid mosaic model of the structure of cell membranes. Science 1972; 175:720–731.
7. Simons K, Ikonen E. Functional rafts in cell membranes. Nature 1997; 387:569–572.
8. Shogomori H, Brown DA. Use of detergents to study membrane rafts: the good, the bad, and the ugly. Biol Chem 2003; 384:1259–1263.
9. Dhungana S, Merrick BA, Tomer KB, Fessler MB. Quantitative proteomics analysis of macrophage rafts reveals compartmentalized activation of the proteasome and of proteasome-mediated ERK activation in response to lipopolysaccharide. Mol Cell Proteomics 2009; 8(1):201–213.
10. Di Girolamo F, Raggi C, Birago C, Pizzi E, Lalle M, Picci L, Pace T, Bachi A, de Jong J, Janse CJ, Waters AP, Sargiacomo M, et al. Plasmodium lipid rafts contain proteins implicated in vesicular trafficking and signalling as well as members of the PIR superfamily, potentially implicated in host immune system interactions. Proteomics 2008; 8:2500–2513.
11. Bernocco S, Fondelli C, Matteoni S, Magnoni L, Gotta S, Terstappen GC, Raggiaschi R. Sequential detergent fractionation of primary neurons for proteomics studies. Proteomics 2008; 8:930–938.
12. Kobayashi M, Katagiri T, Kosako H, Iida N, Hattori S. Global analysis of dynamic changes in lipid raft proteins during T-cell activation. Electrophoresis 2007; 28:2035–2043.
13. Gupta N, Wollscheid B, Watts JD, Scheer B, Aebersold R, DeFranco AL. Quantitative proteomic analysis of B cell lipid rafts reveals that ezrin

regulates antigen receptor-mediated lipid raft dynamics. Nat Immunol 2006; 7:625–633.
14. Roda O, Chiva C, Espuna G, Gabius HJ, Real FX, Navarro P, Andreu D. A proteomic approach to the identification of new tPA receptors in pancreatic cancer cells. Proteomics 2006; 6(suppl 1):S36–S41.
15. Brown DA, Rose JK. Sorting of GPI-anchored proteins to glycolipid-enriched membrane subdomains during transport to the apical cell surface. Cell 1992; 68:533–544.
16. Simons K, Toomre D. Lipid rafts and signal transduction. Nat Rev Mol Cell Biol 2000; 1:31–39.
17. Meiri KF. Membrane/cytoskeleton communication. Subcell Biochem 2004; 37:247–282.
18. Langhorst MF, Reuter A, Luxenhofer G, Boneberg EM, Legler DF, Plattner H, Stuermer CA. Preformed reggie/flotillin caps: stable priming platforms for macrodomain assembly in T cells. FASEB J 2006; 20:711–713.
19. Cross NL. Reorganization of lipid rafts during capacitation of human sperm. Biol Reprod 2004; 71:1367–1373.
20. Sleight SB, Miranda PV, Plaskett NW, Maier B, Lysiak J, Scrable H, Herr JC, Visconti PE. Isolation and proteomic analysis of mouse sperm detergent-resistant membrane fractions: evidence for dissociation of lipid rafts during capacitation. Biol Reprod 2005; 73:721–729.
21. Shadan S, James PS, Howes EA, Jones R. Cholesterol efflux alters lipid raft stability and distribution during capacitation of boar spermatozoa. Biol Reprod 2004; 71:253–265.
22. van Gestel RA, Brewis IA, Ashton PR, Helms JB, Brouwers JF, Gadella BM. Capacitation-dependent concentration of lipid rafts in the apical ridge head area of porcine sperm cells. Mol Hum Reprod 2005; 11:583–590.
23. Selvaraj V, Buttke DE, Asano A, McElwee JL, Wolff CA, Nelson JL, Klaus AV, Hunnicutt GR, Travis AJ. GM1 dynamics as a marker for membrane changes associated with the process of capacitation in murine and bovine spermatozoa. J Androl 2007; 28:588–599.
24. Bou Khalil M, Chakrabandhu K, Xu H, Weerachatyanukul W, Buhr M, Berger T, Carmona E, Vuong N, Kumarathasan P, Wong PT, Carrier D, Tanphaichitr N. Sperm capacitation induces an increase in lipid rafts having zona pellucida binding ability and containing sulfogalactosylglycerolipid. Dev Biol 2006; 290:220–235.
25. Eddy EM, O'Brien DA. The spermatozoon. In: Knobil E, Neill JD (eds.), The Physiology of Reproduction, vol. 1, 2nd ed. New York: Raven Press; 1994:29–77.
26. Suzuki F, Yanagimachi R. Changes in the distribution of intramembranous particles and filipin-reactive membrane sterols during in vitro capacitation of golden hamster spermatozoa. Gamete Res 1989; 23:335–347.
27. Lin Y, Kan FW. Regionalization and redistribution of membrane phospholipids and cholesterol in mouse spermatozoa during in vitro capacitation. Biol Reprod 1996; 55:1133–1146.
28. Hernandez-Gonzalez EO, Sosnik J, Edwards J, Acevedo JJ, Mendoza-Lujambio I, Lopez-Gonzalez I, Demarco I, Wertheimer E, Darszon A, Visconti PE. Sodium and epithelial sodium channels participate in the regulation of the capacitation-associated hyperpolarization in mouse sperm. J Biol Chem 2006; 281(9):5623–5633.
29. Jha KN, Salicioni AM, Arcelay E, Chertihin O, Kumari S, Herr JC, Visconti PE. Evidence for the involvement of proline-directed serine/threonine phosphorylation in sperm capacitation. Mol Hum Reprod 2006; 12:781–789.
30. Treviño CL, Serrano CJ, Beltran C, Felix R, Darszon A. Identification of mouse trp homologs and lipid rafts from spermatogenic cells and sperm. FEBS Lett 2001; 509:119–125.
31. van Gestel RA, Helms JB, Brouwers JF, Gadella BM. Effects of methyl-beta-cyclodextrin-mediated cholesterol depletion in porcine sperm compared to somatic cells. Mol Reprod Dev 2005; 72:386–395.
32. Selvaraj V, Asano A, Buttke DE, McElwee JL, Nelson JL, Wolff CA, Merdiushev T, Fornes MW, Cohen AW, Lisanti MP, Rothblat GH, Kopf GS, et al. Segregation of micron-scale membrane sub-domains in live murine sperm. J Cell Physiol 2006; 206:636–646.
33. Buttke DE, Nelson JL, Schlegel PN, Hunnicutt GR, Travis AJ. Visualization of GM1 with cholera toxin B in live epididymal versus ejaculated bull, mouse, and human spermatozoa. Biol Reprod 2006; 74:889–895.
34. Boesze-Battaglia K. Isolation of membrane rafts and signaling complexes. Methods Mol Biol 2006; 332:169–179.
35. Fujita A, Cheng J, Hirakawa M, Furukawa K, Kusunoki S, Fujimoto T. Gangliosides GM1 and GM3 in the living cell membrane form clusters susceptible to cholesterol depletion and chilling. Mol Biol Cell 2007; 18:2112–2122.
36. Janich P, Corbeil D. GM1 and GM3 gangliosides highlight distinct lipid microdomains within the apical domain of epithelial cells. FEBS Lett 2007; 581:1783–1787.
37. Gomez-Mouton C, Abad JL, Mira E, Lacalle RA, Gallardo E, Jimenez-Baranda S, Illa I, Bernad A, Manes S, Martinez AC. Segregation of leading-edge and uropod components into specific lipid rafts during T cell polarization. Proc Natl Acad Sci U S A 2001; 98:9642–9647.
38. Jung KY, Kim BH, Hwang MR, Cho JR, Kim HM, Lee YC, Kim CH, Kim JK, Kim BJ, Choo YK. Differential distribution of ganglioside GM3 in seminiferous tubule and epididymis of adult rats. Arch Pharm Res 2001; 24:360–366.
39. Bushway AA, Clegg ED, Keenan TW. Composition and synthesis of gangliosides in bovine testis, sperm and seminal plasma. Biol Reprod 1977; 17:432–442.
40. Gore PJ, Singh SP, Brooks DE. Composition of gangliosides from ovine testis and spermatozoa. Biochim Biophys Acta 1986; 876:36–47.
41. Mack SR, Zaneveld LJ, Peterson RN, Hunt W, Russell LD. Characterization of human sperm plasma membrane: glycolipids and polypeptides. J Exp Zool 1987; 243:339–346.
42. Kotani M, Ozawa H, Kawashima I, Ando S, Tai T. Generation of one set of monoclonal antibodies specific for a-pathway ganglio-series gangliosides. Biochim Biophys Acta 1992; 1117:97–103.
43. Kotani M, Terashima T, Tai T. Developmental changes of ganglioside expressions in postnatal rat cerebellar cortex. Brain Res 1995; 700:40–58.
44. Garofalo T, Misasi R, Mattei V, Giammarioli AM, Malorni W, Pontieri GM, Pavan A, Sorice M. Association of the death-inducing signaling complex with microdomains after triggering through CD95/Fas: evidence for caspase-8-ganglioside interaction in T cells. J Biol Chem 2003; 278:8309–8315.
45. Mattei V, Garofalo T, Misasi R, Circella A, Manganelli V, Lucania G, Pavan A, Sorice M. Prion protein is a component of the multimolecular signaling complex involved in T cell activation. FEBS Lett 2004; 560:14–18.
46. Sohn H, Kim YS, Kim HT, Kim CH, Cho EW, Kang HY, Kim NS, Kim CH, Ryu SE, Lee JH, Ko JH. Ganglioside GM3 is involved in neuronal cell death. FASEB J 2006; 20:1248–1250.
47. Chen Y, Qin J, Chen ZW. Fluorescence-topographic NSOM directly visualizes peak-valley polarities of GM1/GM3 rafts in cell membrane fluctuations. J Lipid Res 2008; 49:2268–2275.
48. Ryazantsev S, Yu WH, Zhao HZ, Neufeld EF, Ohmi K. Lysosomal accumulation of SCMAS (subunit c of mitochondrial ATP synthase) in neurons of the mouse model of mucopolysaccharidosis III B. Mol Genet Metab 2007; 90:393–401.
49. Pike LJ. Lipid rafts: heterogeneity on the high seas. Biochem J 2004; 378:281–292.
50. Okabe M, Adachi T, Takada K, Oda H, Yagasaki M, Kohama Y, Mimura T. Capacitation-related changes in antigen distribution on mouse sperm heads and its relation to fertilization rate in vitro. J Reprod Immunol 1987; 11:91–100.
51. Kawai Y, Hama T, Mayumi T, Okabe M, Matzno S, Kohama Y, Mimura T. Flow cytometric analysis of mouse sperm using monoclonal anti-sperm antibody OBF13. J Reprod Immunol 1989; 16:71–82.
52. Myles DG, Primakoff P. Localized surface antigens of guinea pig sperm migrate to new regions prior to fertilization. J Cell Biol 1984; 99:1634–1641.
53. Rochwerger L, Cuasnicu PS. Redistribution of a rat sperm epididymal glycoprotein after in vitro and in vivo capacitation. Mol Reprod Dev 1992; 31:34–41.
54. Jones R, James PS, Howes L, Bruckbauer A, Klenerman D. Supramolecular organization of the sperm plasma membrane during maturation and capacitation. Asian J Androl 2007; 9:438–444.
55. Inoue N, Ikawa M, Isotani A, Okabe M. The immunoglobulin superfamily protein Izumo is required for sperm to fuse with eggs. Nature 2005; 434:234–238.
56. Zaas DW, Duncan M, Rae Wright J, Abraham SN. The role of lipid rafts in the pathogenesis of bacterial infections. Biochim Biophys Acta 2005; 1746:305–313.
57. Wang H, Yang P, Liu K, Guo F, Zhang Y, Zhang G, Jiang C. SARS coronavirus entry into host cells through a novel clathrin- and caveolae-independent endocytic pathway. Cell Res 2008; 18:290–301.
58. Hazarika P, McCarty MF, Prieto VG, George S, Babu D, Koul D, Bar-Eli M, Duvic M. Up-regulation of Flotillin-2 is associated with melanoma progression and modulates expression of the thrombin receptor protease activated receptor 1. Cancer Res 2004; 64:7361–7369.
59. Kawamura S, Ohyama C, Watanabe R, Satoh M, Saito S, Hoshi S, Gasa S, Orikasa S. Glycolipid composition in bladder tumor: a crucial role of GM3 ganglioside in tumor invasion. Int J Cancer 2001; 94:343–347.